Journal of
Instrumentation

OPEN ACCESS

B flavour tagging using charm decays at the LHCb experiment

To cite this article: The LHCb collaboration 2015 *JINST* **10** P10005

View the article online for updates and enhancements.

You may also like

- Statistical mechanics of logarithmic REM: duality, freezing and extreme value statistics of 1/*f* noises generated by Gaussian free fields
Yan V Fyodorov, Pierre Le Doussal and Alberto Rosso
- An effective field theory model for one-dimensional CH chains: effects at finite chemical potential, temperature and external Zeeman magnetic field
Heron Caldas
- The LHCb Upgrade I
R. Aaij, A.S.W. Abdelmotteleb, C. Abellan Beteta et al.

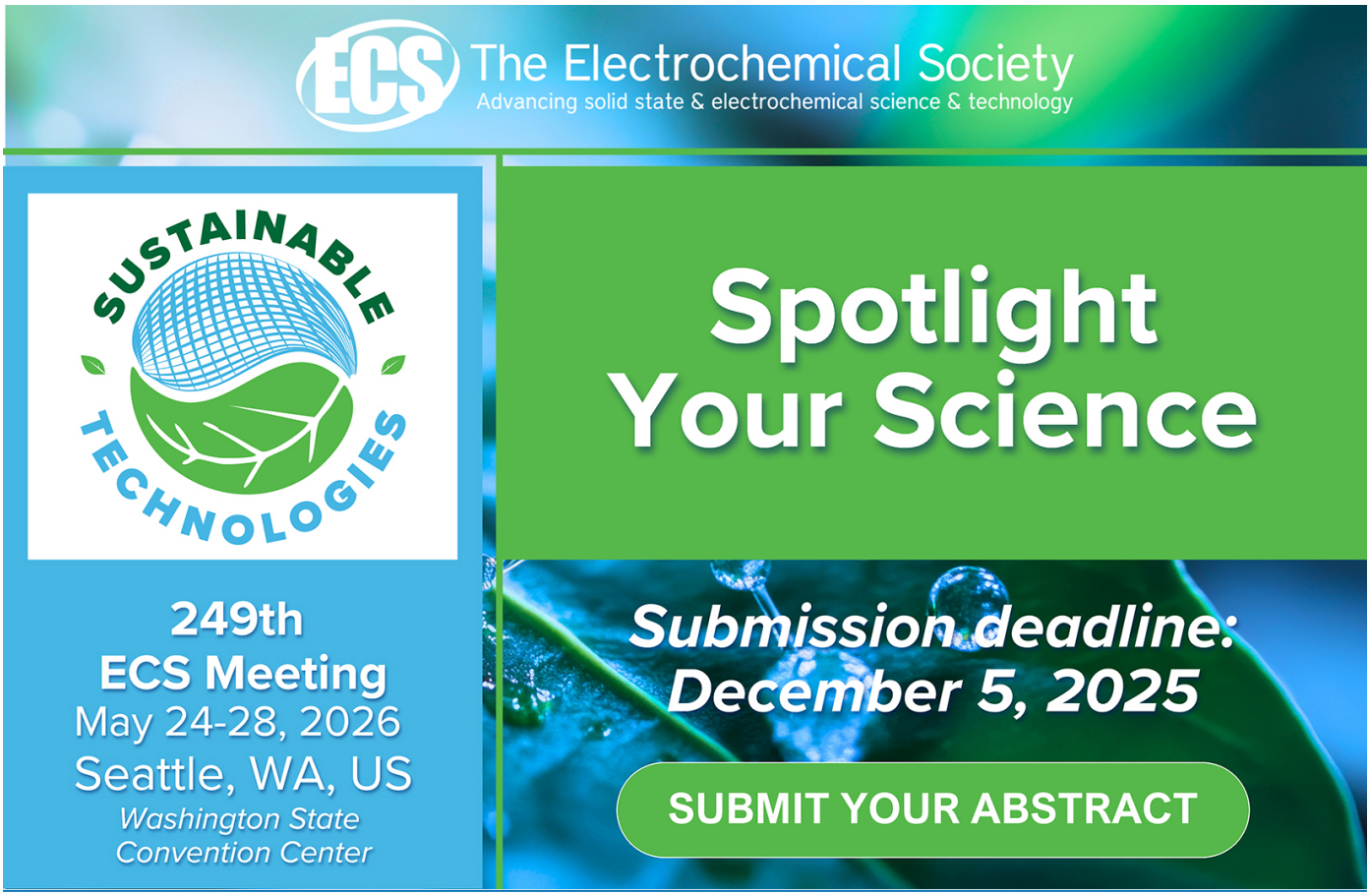

This content was downloaded from IP address 84.226.37.59 on 08/11/2025 at 17:04

PUBLISHED BY IOP PUBLISHING FOR SISSA MEDIALAB

RECEIVED: *August 3, 2015*
ACCEPTED: *August 29, 2015*
PUBLISHED: *October 5, 2015*

B flavour tagging using charm decays at the LHCb experiment

The LHCb collaboration

E-mail: jwimberl@cern.ch

ABSTRACT: An algorithm is described for tagging the flavour content at production of neutral B mesons in the LHCb experiment. The algorithm exploits the correlation of the flavour of a B meson with the charge of a reconstructed secondary charm hadron from the decay of the other b hadron produced in the proton-proton collision. Charm hadron candidates are identified in a number of fully or partially reconstructed Cabibbo-favoured decay modes. The algorithm is calibrated on the self-tagged decay modes $B^+ \to J/\psi K^+$ and $B^0 \to J/\psi K^{*0}$ using $3.0\,\text{fb}^{-1}$ of data collected by the LHCb experiment at pp centre-of-mass energies of 7 TeV and 8 TeV. Its tagging power on these samples of $B \to J/\psi X$ decays is $(0.30 \pm 0.01 \pm 0.01)\%$.

KEYWORDS: Performance of High Energy Physics Detectors; Analysis and statistical methods

ARXIV EPRINT: 1507.07892

© CERN 2015 for the benefit of the LHCb collaboration, published under the terms of the Creative Commons Attribution 3.0 License by IOP Publishing Ltd and Sissa Medialab srl. Any further distribution of this work must maintain attribution to the author(s) and the published article's title, journal citation and DOI.

doi:10.1088/1748-0221/10/10/P10005

2015 JINST 10 P10005

Contents

1 Introduction 1

2 Detector and simulation 2

3 Tagging potential of OS charm hadrons 3

4 Selection of charm candidates 3

5 Calibration 5

6 Performance 8

7 Conclusion 9

The LHCb collaboration 12

2015 JINST 10 P10005

1 Introduction

Measurements that involve mixing and time-dependent *CP* asymmetries in decays of neutral B mesons require the identification of their flavour content at production. This is achieved via various flavour tagging algorithms that exploit information from the rest of the pp collision event. Same-side (SS) taggers look for particles produced in association with the signal B meson during the hadronization of the b quark [1]. The d or s partner of the light valence quark of the signal B has a roughly 50% chance of hadronizing into a charged pion or kaon. Since b quarks are mostly produced in $b\bar{b}$ pairs, the flavour content of the signal B meson can also be deduced from available information on the opposite-side (OS) b hadron, whose flavour is the opposite of the signal B meson at the production time. OS muon and electron taggers look for leptons originating from semileptonic $b \to cW$ transitions of the b hadron, and an OS kaon tagger looks for kaons coming from $b \to c \to s$ transitions. A vertex-charge tagger reconstructs the decay vertex of the OS b hadron and predicts its charge by weighting the charges of its decay products according to their transverse momentum. The OS taggers employed by LHCb are described in ref. [2] and the SS taggers in refs. [3, 4]. This paper reports a new flavour tagging algorithm for the LHCb experiment that relies on reconstructed decays of charm hadrons produced in the OS b hadron decay. For the development and evaluation of the tagging algorithm, signal B meson and charm hadron candidates are reconstructed using data from $3\,\text{fb}^{-1}$ of integrated luminosity collected by LHCb at 7 TeV and 8 TeV centre-of-mass energies in 2011 and 2012, respectively.

The performance of a flavour tagging algorithm is defined by its tagging efficiency, ε_{tag}, mistag fraction, ω, and dilution, $\mathcal{D} = 1 - 2\omega$. For a simple tagging algorithm with discrete decisions – B^0, $\bar{B}^0$, or untagged – these metrics are directly related to the numbers of rightly tagged (R), wrongly tagged (W), and untagged events (U) in a signal sample:

$$\varepsilon_{\text{tag}} = \frac{R+W}{R+W+U}, \quad \omega = \frac{W}{R+W}, \quad \mathcal{D} = \frac{R-W}{R+W}. \tag{1.1}$$

The performance of the flavour tagging algorithms is improved by assigning confidence weights to their tagging decisions. For each tagger, a multivariate classifier is trained using simulated data to distinguish between correct and incorrect decisions [2]. The inputs to the classifier are a selection of kinematic and geometric quantities describing the tagging track(s), the signal B meson, and the event. This classifier then calculates a predicted mistag probability η for each decision made. The predicted mistag probability is calibrated to data using an appropriate flavour self-tagged mode, such as $B^+ \to J/\psi K^+$, or a mode involving neutral B oscillation, which self-tags its flavour at the decay-time, such as $B^0 \to J/\psi K^{*0}$ or $B_s^0 \to D_s^- \pi^+$ [4, 5] (the use of charge-conjugate modes is implied throughout this paper). This calibration procedure provides a function $\omega(\eta)$, which relates the actual mistag probability ω to the predicted mistag probability η. Weighting each signal candidate by $1-2\omega(\eta)$ leads to an improved effective mistag fraction ω and associated dilution $\mathcal{D} = 1-2\omega$. The statistical power of a *CP* asymmetry measurement using a tagging algorithm is proportional to the effective tagging efficiency (or tagging power) ε_{eff}, defined as

$$\varepsilon_{\text{eff}} = \varepsilon_{\text{tag}}\mathcal{D}^2. \tag{1.2}$$

The typical combined tagging power of the current set of OS tagging algorithms used by LHCb is approximately 2.5% [3, 6–8]. Any augmentation to this tagging power increases the statistical precision achievable in *CP* measurements at LHCb.

2 Detector and simulation

The LHCb detector [9, 10] is a single-arm forward spectrometer covering the pseudorapidity range between 2 and 5, designed for the study of particles containing b or c quarks. The detector includes a high-precision tracking system consisting of a silicon-strip vertex detector surrounding the pp interaction region [11], a large-area silicon-strip detector located upstream of a dipole magnet with a bending power of about 4 Tm, and three stations of silicon-strip detectors and straw drift tubes [12] placed downstream of the magnet. The tracking system provides a measurement of momentum, p, of charged particles with a relative uncertainty that varies from 0.5% at low momentum to 1.0% at 200 GeV/c. The minimum distance of a track to a primary vertex (PV), the impact parameter, is measured with a resolution of $(15+29/p_{\text{T}})\,\mu$m, where p_{T} is the component of the momentum transverse to the beam, in GeV/c. Different types of charged hadrons in the momentum range 2–100 GeV/c are distinguished using information from two ring-imaging Cherenkov detectors [13]. Photons, electrons and hadrons are identified by a calorimeter system consisting of scintillating-pad and preshower detectors, an electromagnetic calorimeter and a hadronic calorimeter. Muons are identified by a system composed of alternating layers of iron and multiwire proportional chambers [14]. The online event selection is performed by a trigger [15], which consists of a hardware stage, based on information from the calorimeter and muon systems, followed by a software stage, which applies a full event reconstruction.

In the simulation, pp collisions are generated using PYTHIA [16, 17] with a specific LHCb configuration [18]. Decays of hadronic particles are described by EVTGEN [19], in which final-state radiation is generated using PHOTOS [20]. The interaction of the generated particles with the detector, and its response, are implemented using the GEANT4 toolkit [21] as described in ref. [22].

2015 JINST 10 P10005

3 Tagging potential of OS charm hadrons

In events containing a signal B decay, the opposite-side D^+, D^0, and Λ_c^+ charm hadrons are primarily produced through the quark-level $b \to c$ transition. The charge of the D^+ or Λ_c^+ determines the flavour of the b hadron parent. For D^0 decays through the dominant Cabibbo-favoured process $D^0 \to K^- X$, the kaon charge determines the flavour of the charm hadron, and thereby that of the parent B hadron (the effect of D^0 mixing is negligible). The OS charm tagging algorithm uses charm hadron candidates reconstructed in a number of decay modes, chosen for their relatively large branching fractions, listed in table 1. These include fully reconstructed hadronic modes with a single charged kaon in the final state, partially reconstructed hadronic modes with an unobserved neutral pion, and partially reconstructed semileptonic modes. Table 1 also reports the breakdown of the charm tagger's performance by decay mode. The relative rate and relative power of each mode are the amounts that it contributes to the algorithm's total tagging rate ε_{tag} and tagging power ε_{eff}, which are presented in section 6 and table 3. The algorithm predicts the flavour of the signal B meson using the charge of the kaon in the same manner as the OS kaon tagger; however, the selection based on the reconstruction of c hadrons (rather than the selection of kaons based on their individual kinematic properties) results in a different set of selected kaons and provides a complementary source of tagging information.

Several effects contribute an irreducible component to the mistag probability for the OS charm tagging algorithm. The dominant impact comes from B^0–$\bar{B}^0$ oscillation and from the contributions of "wrong sign" charm hadrons produced in $b \to c\bar{c}q$ transitions. The impact of Cabibbo-suppressed $D^0 \to K^+ X$ decays is negligible, as these typically produce additional kaons and do not mimic modes used by the tagging algorithm, and doubly Cabibbo-suppressed decays such as $D^0 \to K^+\pi^-$ have a negligibly small branching fraction. Accounting for relative production rates of b hadrons, neutral B oscillation, and branching fractions of the decay modes used in the tagger, the irreducible mistag probabilities for D^0, D^+ and Λ_c^+ modes are estimated to be 23%, 19%, and 6%, respectively.

In addition to the irreducible mistag probability arising from physics effects, the charm hadron candidates are contaminated by combinatorial and partially reconstructed b and c hadron background that can lead to an incorrect flavour tag result. For each mode, the charm tagger uses a multivariate algorithm that combines geometric and kinematic quantities and properties of the c hadron candidate and its daughters. The resulting discriminating variable is used both to suppress the combinatorial background and to predict the corresponding mistag probability for the surviving candidate.

4 Selection of charm candidates

Charm decay candidates are formed by combining kaon, pion, and proton candidates that satisfy particle identification criteria. These particles are required to have momentum $p > 1000\,\text{MeV}/c$, transverse momentum with respect to the beam axis $p_{\text{T}} > 100\,\text{MeV}/c$, and to be significantly displaced from any PV. For the candidates in the partially reconstructed modes and the decay $D^0 \to K^-\pi^+\pi^+\pi^-$, which contain large combinatorial backgrounds, more stringent requirements are imposed on the displacement of the final-state particles from the PV. In addition, particles are required to have $p_{\text{T}} > 150\,\text{MeV}/c$ for candidates in the mode $D^0 \to K^-\pi^+\pi^+\pi^-$.

2015 JINST 10 P10005

Table 1. Decay modes used in the OS charm tagger. The symbol H_c stands for any c hadron. The definition of the two right-most columns is given in the text.

Decay mode	Relative rate	Relative power
$D^0 \to K^-\pi^+$	10.0%	24.0%
$D^0 \to K^-\pi^+\pi^+\pi^-$	5.9%	8.4%
$D^+ \to K^-\pi^+\pi^+$	10.3%	2.6%
$H_c \to K^-\pi^+X$	69.7%	61.5%
$H_c \to K^-e^+X$	0.5%	0.2%
$H_c \to K^-\mu^+X$	3.4%	0.3%
$\Lambda_c^+ \to p^+K^-\pi^+$	0.2%	2.4%

Charm hadron candidates are required to pass a number of selection requirements. These include a maximum distance of closest approach between each pair of daughter tracks and a minimum quality of the decay vertex fit. Each candidate is required to be well separated from any PV and to have a trajectory that leads back to the best PV, chosen to be the PV for which the impact parameter significance of the charm hadron is smallest. The invariant mass of the charm hadron candidate is required to be consistent with the known mass of the corresponding charm hadron, within $100\,\mathrm{MeV}/c^2$ for the Λ_c^+ channel and $50\,\mathrm{MeV}/c^2$ for all other fully reconstructed D decay modes. For the partially reconstructed $D \to K^-\pi^+X$ modes, the $K^-\pi^+$ mass is required to be in a $\left[-400\,\mathrm{MeV}/c^2, +0\,\mathrm{MeV}/c^2\right]$ window around the known D^0 mass or in a window of $\pm 50\,\mathrm{MeV}/c^2$ around the $K^*(892)^0$ resonance. The former is favoured by the invariant mass distribution of $K^-\pi^+$ pairs from the quasi-two body decay $D^0 \to K^-\rho^+$, and the latter selects $D \to K^*(892)^0X$ decays. Charm candidates surviving these criteria still contain significant background contamination, which must be further reduced in order to lower the mistag probability of the algorithm.

For each mode, an adaptive-boosted decision tree (BDT) [23, 24] is used both to suppress background candidates and to estimate mistag probabilities. The inputs to the BDT are variables describing the decay kinematics, decay vertex and displacement, and particle identification information on the decay products. A variable related to the decay-time is calculated from the distance between the c hadron's decay vertex and the corresponding best PV; this approximates the sum of the decay-times of the c hadron and its parent b hadron. The BDT algorithms are trained using Monte Carlo (MC) simulations of $b\bar{b}$ events containing $B^+ \to J/\psi K^+$, $B^0 \to J/\psi K^{*0}$, and $B_s^0 \to J/\psi\,\phi$ decays on the signal side and inclusive decays of the b hadron on the opposite-side. These B decays are used to model the various sources and amounts of background when reconstructing OS c hadrons recoiling against signal B decays.

The output of the BDT, along with the simulation record of candidate identification, is used to compute the predicted mistag probability η for each c hadron candidate. Candidates with $\eta < 45\%$ are used in the flavour tagging decision. Removing candidates that fail this criterion significantly reduces the computing time of the algorithm at little cost to tagging performance. In cases where multiple charm candidates are present, the candidate with the lowest predicted mistag probability is retained. The combined efficiency of these requirements for retaining tagged events is $(59.00 \pm 0.07)\%$ and $(53.4 \pm 0.3)\%$ in simulation and data, respectively.

2015 JINST 10 P10005

5 Calibration

While simulated data are used to develop and optimize the charm tagging algorithm, its performance is calibrated with collision data by comparing the algorithm's predictions to the known flavours of signal B candidates, according to the procedure detailed in ref. [2]. The calibration parameters p_0, p_1, Δp_0, and Δp_1 are defined by

$$\omega = p_0 + p_1\,(\eta - \langle\eta\rangle)$$
$$\Delta\omega = \Delta p_0 + \Delta p_1\,(\eta - \langle\eta\rangle)$$

where $\langle\eta\rangle$ is the average predicted mistag probability, ω is the actual mistag probability averaged over B^+ and B^- signal mesons, and $\Delta\omega$ is the excess mistag probability for B^+ mesons with respect to B^- mesons; equivalent definitions hold for $B^0/\bar{B}^0$ signal. In the ideal case, the offset parameter p_0 should equal $\langle\eta\rangle$, and so the related parameter $\delta p_0 = p_0 - \langle\eta\rangle$ is often more convenient.

A calibration of the algorithm has been performed using the flavour self-tagged mode $B^+ \to J/\psi K^+$. The signal candidates are selected by combining pairs of oppositely charged muons, with invariant mass consistent with the known J/ψ mass, with charged kaons, and are required to pass a set of cuts to obtain a good signal to background ratio [2]. When multiple candidates are present for a single event, that with the best decay vertex fit is kept. A fit to the reconstructed B^+ mass distribution is used to separate signal and background via the *sPlot* procedure, which computes signal and background weights for each candidate [25]. The empirical model for the signal is a sum of two Crystal Ball functions [26], while background is modeled by an exponential distribution. A total of 1.1×10^6 signal candidates in this channel are found in the full dataset. The parameters p_0 and p_1 are determined by splitting the data into 13 bins of η between 0.19 and 0.45, calculating ω_i and $\bar{\eta}_i$ (the average η) in each bin, and performing a linear fit to the set of values $(\omega_i, \bar{\eta}_i)$. The calibration parameters Δp_0 and Δp_1 are obtained from fits to the B^+ and B^- data each split into 5 bins of η. The quantities $\Delta\omega_i$ and $\bar{\eta}_i$ are calculated in each of the 5 bins, and a linear fit is performed to the set of values $(\Delta\omega_i, \bar{\eta}_i)$. These fits are shown in Figs. 1 and 2. The resulting calibration parameters are given in table 2.

A cross-check of the calibration has been carried out using a $B^0 \to J/\psi K^{*0}$ control sample. For this calibration, B^0–$\bar{B}^0$ oscillation must be taken into account. The Hypatia function [27] is used to model the signal's mass distribution, while the background is modeled with a sum of two exponential functions. A set of simultaneous fits to the B^0 lifetime distribution in bins of η is performed, in which p_0, p_1, Δp_0, and Δp_1 are parameters of the fit model. In each bin, the raw B^0–$\bar{B}^0$ mixing asymmetry is defined as

$$\mathcal{A}_{\text{mixing}} = \frac{\mathcal{N}(\mathcal{D} = \mathcal{P}) - \mathcal{N}(\mathcal{D} \neq \mathcal{P})}{\mathcal{N}(\mathcal{D} = \mathcal{P}) + \mathcal{N}(\mathcal{D} \neq \mathcal{P})}, \tag{5.1}$$

where $\mathcal{D}$ is the B meson flavour at decay-time and $\mathcal{P}$ is the production flavour predicted by the charm tagger. The amplitude of this asymmetry is governed by the actual mistag fraction ω_i in the bin, while the bin's average predicted mistag probability is $\bar{\eta}_i$. The fit attempts to match the calibrated value $\omega(\bar{\eta}_i)$ to ω_i in each bin by adjusting the calibration parameters. A projection of the fitted model to the mixing asymmetry is shown in Fig. 3. The values of the calibration parameters obtained from the fit are given in table 2. The parameters are compatible with those obtained in the $B^+ \to J/\psi K^+$ mode, with the total χ^2 per degree of freedom equal to 0.65.

2015 JINST 10 P10005

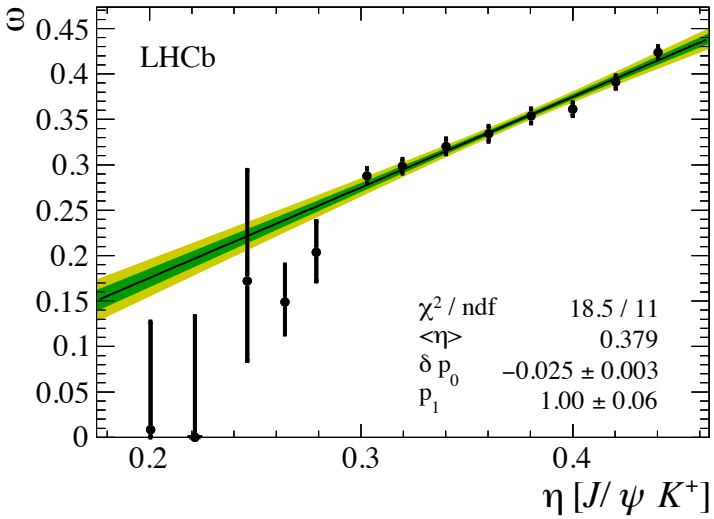

Figure 1. Mistag probability ω as a function of the predicted mistag probability η for the $B^+ \to J/\psi K^+$ data sample. A straight line fit to extract the parameters p_0 and p_1 is superimposed. The dark (green) and light (yellow) bands are the regions within 1σ and 2σ of the fitted value, respectively.

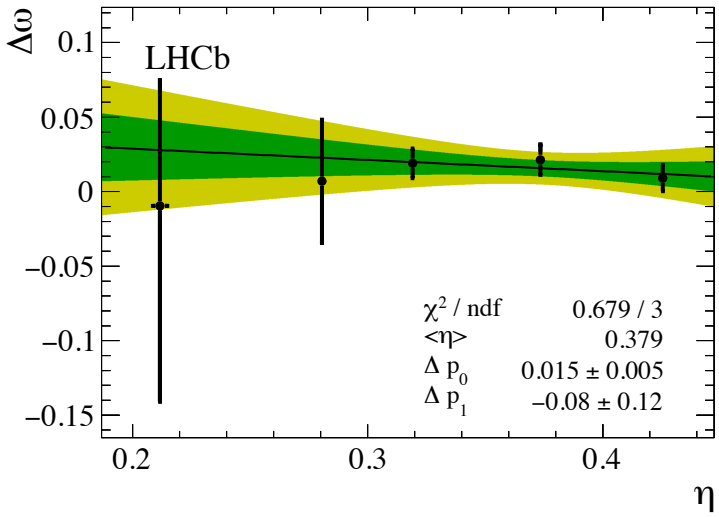

Figure 2. Excess mistag probability $\Delta\omega$ as a function of the predicted mistag probability η for the $B^+ \to J/\psi K^+$ data sample. A straight line fit to extract the parameters Δp_0 and Δp_1 is superimposed. The dark (green) and light (yellow) bands are the regions within 1σ and 2σ of the fitted value, respectively.

2015 JINST 10 P10005

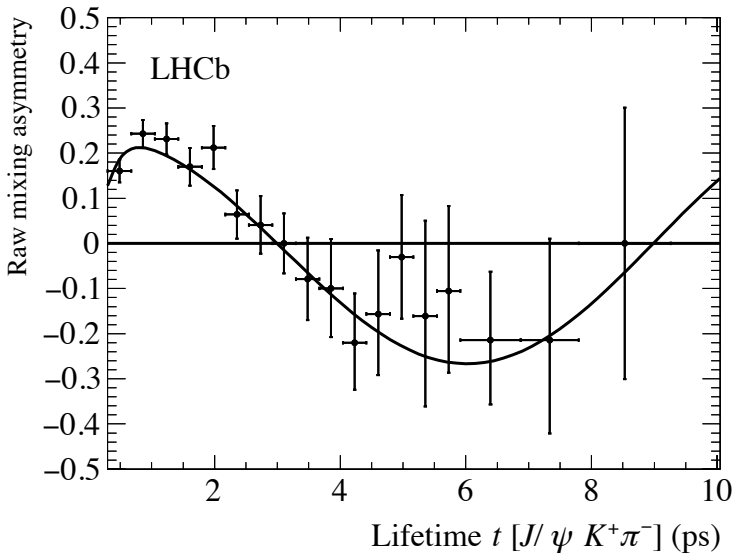

Figure 3. Raw B^0–$\bar{B}^0$ mixing asymmetry (defined in eq. 5.1) vs. decay-time for the $B^0 \to J/\psi K^{*0}$ data sample. The amplitude of the asymmetry is diluted due to mistagging by the charm tagger. The mixing asymmetry from the fit is superimposed.

Table 2. Calibration parameters as determined from the $B^+ \to J/\psi K^+$ and $B^0 \to J/\psi K^{*0}$ control samples. For both calibration modes, the average predicted mistag probability $\langle\eta\rangle$ is 0.379. The first uncertainties are statistical and the second are systematic. The systematic uncertainties are evaluated using simulation.

Sample	δp_0 (10^{-3})	p_1	Δp_0 (10^{-3})	Δp_1
$B^+ \to J/\psi K^+$	$-25 \pm 3 \pm 3$	$1.00 \pm 0.06 \pm 0.02$	$15 \pm 5 \pm 4$	$-0.08 \pm 0.12 \pm 0.04$
$B^0 \to J/\psi K^{*0}$	$-18 \pm 8 \pm 3$	$1.16 \pm 0.17 \pm 0.02$	$23 \pm 11 \pm 4$	$0.21 \pm 0.25 \pm 0.04$

The relatively small yield of the decay $B_s^0 \to D_s^- \pi^+$ precludes performing a data-driven calibration on a B_s^0 mode. Therefore, in order to ensure that the algorithm performs similarly for B_s^0 channels as well as B^+ and B^0 channels, separate calibrations to simulated $B^+ \to J/\psi K^+$, $B^0 \to J/\psi K^{*0}$, and $B_s^0 \to J/\psi \phi$ events are performed. Where statistically significant differences between the calibration parameters in the three channels are found, a systematic uncertainty, corresponding to half of the maximum difference, is assigned to the parameter. These systematic uncertainties are roughly the size of the statistical uncertainties for the parameters p_0 and Δp_0, but are negligible for p_1 and Δp_1. The propagation of these uncertainties results in a 0.011% absolute systematic uncertainty on the tagging power, comparable to its statistical uncertainty.

Other sources of systematic uncertainty on calibration parameters have been investigated and found to have negligible effect. These include the potential effect of the chosen model of the invariant B mass distribution for the channel $B^+ \to J/\psi K^+$. Two alternative models of the mass distribution were used and gave nearly identical results.

There are additional systematic uncertainties related to flavour tagging that must be considered in a *CP* asymmetry analysis. These include differences between the signal channel sample and calibration channel sample in phase space distribution, event multiplicity, number of primary vertices,

2015 JINST 10 P10005

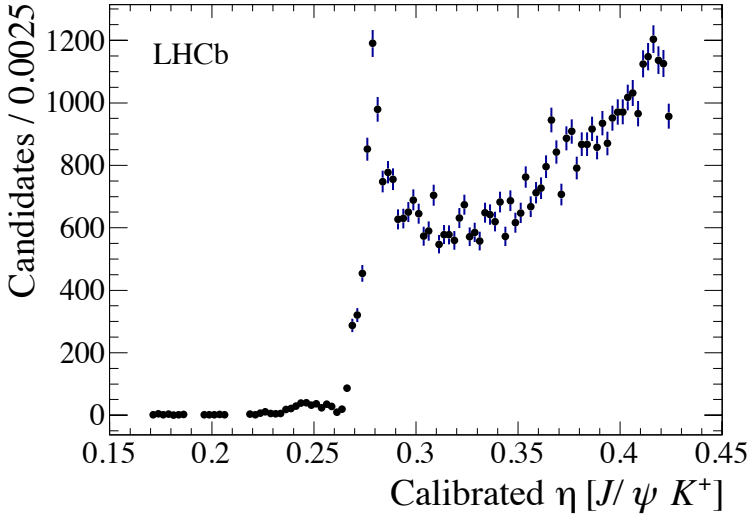

Figure 4. Distribution of the calibrated predicted mistag probability $\omega(\eta)$ for the $B^+ \to J/\psi K^+$ data sample.

Table 3. Tagging efficiencies (ε_{tag}), effective mistag fractions (ω), and tagging powers (ε_{eff}) in the various data samples studied. The first uncertainties are statistical and the second are systematic. The sample labeled Simulation is the training sample of simulated $B^+ \to J/\psi K^+$, $B^0 \to J/\psi K^{*0}$, and $B_s^0 \to J/\psi \phi$ decays, which has negligible statistical uncertainties.

Sample	ε_{tag}	ω	ε_{eff}
Simulation	4.88%	37.0%	0.33%
$B^+ \to J/\psi K^+$	$(3.11 \pm 0.02)\%$	$(34.6 \pm 0.3 \pm 0.3)\%$	$(0.30 \pm 0.01 \pm 0.01)\%$
$B^0 \to J/\psi K^{*0}$	$(3.32 \pm 0.04)\%$	$(35.0 \pm 0.8 \pm 0.3)\%$	$(0.30 \pm 0.03 \pm 0.01)\%$
$B^0 \to D^- \pi^+$	$(4.11 \pm 0.03)\%$	$(34.4 \pm 0.4 \pm 0.3)\%$	$(0.40 \pm 0.02 \pm 0.01)\%$
$B_s^0 \to D_s^- \pi^+$	$(3.99 \pm 0.07)\%$	$(34.4 \pm 0.6 \pm 0.3)\%$	$(0.39 \pm 0.03 \pm 0.01)\%$

or other variables. These differences would require corrections and would introduce tagging-related systematic uncertainties. Such effects are dependent on the signal channel and selection, and must be determined separately for each analysis.

6 Performance

The distribution of η after calibration for the $B^+ \to J/\psi K^+$ control sample is shown in Fig. 4. The tagging efficiency, mistag fraction, and the tagging power of the charm tagger are reported in table 3 for the training sample of simulated $B \to J/\psi X$ decays and for both calibration channels. The propagated statistical uncertainty of the calibration parameters dominates the statistical uncertainty of the tagging power. The overall tagging power is slightly higher in simulation than in data, due to differences in the distributions of input variables. The tagging powers in the two $B \to J/\psi X$ calibration channels are consistent.

Table 3 also reports the tagging metrics for the decays $B^0 \to D^- \pi^+$ and $B_s^0 \to D_s^- \pi^+$. Fits to the mass distributions of the signal candidates are performed to separate signal from background.

2015 JINST 10 P10005

In each fit, the signal is modeled by a sum of two Crystal Ball functions and the combinatorial background is described by an exponential function. Several fully and partially reconstructed backgrounds are also modeled in the fit to the $B_s^0 \to D_s^- \pi^+$ sample. The tagging efficiency for these samples is found to be higher than for the samples of $B \to J/\psi X$ decays, due to correlations between the kinematics of the signal B and the opposite-side charm hadrons. The effective mistag fraction for these samples is consistent with that on the $B \to J/\psi X$ samples. The net effect is an increased tagging power for these $B \to DX$ decays, similar to that observed for other opposite-side tagging algorithms [7, 28].

To use the charm tagger in a physics analysis, the flavour tagging information from the charm tagger can be combined with information from other tagging algorithms. Assessing the actual gain in performance depends on the method of combination and calibration, as well as on the set of tagging algorithms being combined. Due to correlations with other tagging algorithms, in particular the OS kaon and vertex-charge taggers, the maximum possible increase in tagging power after the addition of the charm tagging algorithm is less than its individual tagging power. The performance of the combination of the current OS tagging algorithms with and without the addition of the charm tagger has been measured on the $B^+ \to J/\psi K^+$ data sample. The absolute net gain in tagging power using the current combination algorithm is found to be around 0.11%, compared to the current total OS tagging power of about 2.5% [3, 6–8].

7 Conclusion

An algorithm has been developed that determines the flavour of a signal b hadron at production time by reconstructing opposite-side charm hadrons from a number of decay channels. The flavour tagger uses boosted decision tree algorithms trained on simulated data, and has been calibrated and evaluated on data using the self-tagged decay $B^+ \to J/\psi K^+$. Its tagging power for data in this channel is found to be $(0.30 \pm 0.01\,(\text{stat}) \pm 0.01\,(\text{syst}))\%$. The calibration has been cross-checked using the decay $B^0 \to J/\psi K^{*0}$, giving consistent results. The tagging power is found to be higher for the decays $B^0 \to D^- \pi^+$ and $B_s^0 \to D_s^- \pi^+$, at $(0.40 \pm 0.02\,(\text{stat}) \pm 0.01\,(\text{syst}))\%$ and $(0.39 \pm 0.03\,(\text{stat}) \pm 0.01\,(\text{syst}))\%$, respectively.

Acknowledgments

We express our gratitude to our colleagues in the CERN accelerator departments for the excellent performance of the LHC. We thank the technical and administrative staff at the LHCb institutes. We acknowledge support from CERN and from the national agencies: CAPES, CNPq, FAPERJ and FINEP (Brazil); NSFC (China); CNRS/IN2P3 (France); BMBF, DFG, HGF and MPG (Germany); INFN (Italy); FOM and NWO (The Netherlands); MNiSW and NCN (Poland); MEN/IFA (Romania); MinES and FANO (Russia); MinECo (Spain); SNSF and SER (Switzerland); NASU (Ukraine); STFC (United Kingdom); NSF (USA). The Tier1 computing centres are supported by IN2P3 (France), KIT and BMBF (Germany), INFN (Italy), NWO and SURF (The Netherlands), PIC (Spain), GridPP (United Kingdom). We are indebted to the communities behind the multiple open source software packages on which we depend. We are also thankful for the computing resources and the access to software R&D tools provided by Yandex LLC (Russia). Individual groups

2015 JINST 10 P10005

or members have received support from EPLANET, Marie Skłodowska-Curie Actions and ERC (European Union), Conseil général de Haute-Savoie, Labex ENIGMASS and OCEVU, Région Auvergne (France), RFBR (Russia), XuntaGal and GENCAT (Spain), Royal Society and Royal Commission for the Exhibition of 1851 (United Kingdom).

References

[1] M. Gronau, A. Nippe and J.L. Rosner, *Method for flavor tagging in neutral B meson decays*, *Phys. Rev.* **D 47** (1993) 1988 [hep-ph/9211311].

[2] LHCb collaboration, *Opposite-side flavour tagging of B mesons at the LHCb experiment*, *Eur. Phys. J.* **C 72** (2012) 2022 [arXiv:1202.4979].

[3] LHCb collaboration, *Measurement of CP violation in $B^0 \to J/\psi K^0_S$ decays*, *Phys. Rev. Lett.* **115** (2015) 031601 [arXiv:1503.07089].

[4] LHCb collaboration, *Optimization and calibration of the same-side kaon tagging algorithm using hadronic B^0_s decays in 2011 data*, LHCb-CONF-2012-033 (2012).

[5] LHCb collaboration, *Performance of flavour tagging algorithms optimised for the analysis of $B^0_s \to J/\psi\phi$*, LHCb-CONF-2012-026 (2012).

[6] LHCb collaboration, *Measurement of the CP-violating phase β in $B^0 \to J/\psi\pi^+\pi^-$ decays and limits on penguin effects*, *Phys. Lett.* **B 742** (2015) 38 [arXiv:1411.1634].

[7] LHCb collaboration, *Precision measurement of CP violation in $B^0_s \to J/\psi K^+K^-$ decays*, *Phys. Rev. Lett.* **114** (2015) 041801 [arXiv:1411.3104].

[8] LHCb collaboration, *Measurement of the time-dependent CP asymmetries in $B^0_s \to J/\psi K^0_S$*, *JHEP* **06** (2015) 131 [arXiv:1503.07055].

[9] LHCb collaboration, *The LHCb Detector at the LHC*, 2008 *JINST* **3** S08005.

[10] LHCb collaboration, *LHCb Detector Performance*, *Int. J. Mod. Phys.* **A 30** (2015) 1530022 [arXiv:1412.6352].

[11] R. Aaij et al., *Performance of the LHCb Vertex Locator*, 2014 *JINST* **9** P09007 [arXiv:1405.7808].

[12] LHCb Outer Tracker Group collaboration, R. Arink et al., *Performance of the LHCb Outer Tracker*, 2014 *JINST* **9** P01002 [arXiv:1311.3893].

[13] LHCb RICH Group collaboration, M. Adinolfi et al., *Performance of the LHCb RICH detector at the LHC*, *Eur. Phys. J.* **C 73** (2013) 2431 [arXiv:1211.6759].

[14] A.A. Alves, Jr. et al., *Performance of the LHCb muon system*, 2013 *JINST* **8** P02022 [arXiv:1211.1346].

[15] R. Aaij et al., *The LHCb Trigger and its Performance in 2011*, 2013 *JINST* **8** P04022 [arXiv:1211.3055].

[16] T. Sjöstrand, S. Mrenna and P.Z. Skands, *PYTHIA 6.4 Physics and Manual*, *JHEP* **05** (2006) 026 [hep-ph/0603175].

[17] T. Sjöstrand, S. Mrenna and P.Z. Skands, *A Brief Introduction to PYTHIA 8.1*, *Comput. Phys. Commun.* **178** (2008) 852 [arXiv:0710.3820].

[18] LHCb collaboration, *Handling of the generation of primary events in Gauss, the LHCb simulation framework*, *J. Phys. Conf. Ser.* **331** (2011) 032047.

2015 JINST 10 P10005

[19] D.J. Lange, *The EvtGen particle decay simulation package*, *Nucl. Instrum. Meth.* **A 462** (2001) 152.

[20] P. Golonka and Z. Was, *PHOTOS Monte Carlo: A Precision tool for QED corrections in Z and W decays*, *Eur. Phys. J.* **C 45** (2006) 97 [hep-ph/0506026].

[21] Geant4 collaboration, J. Allison *et al.*, *Geant4 developments and applications*, *IEEE Trans. Nucl. Sci.* **53** (2006) 270.

[22] M. Clemencic et al., *The LHCb simulation application, Gauss: Design, evolution and experience*, *J. Phys. Conf. Ser.* **331** (2011) 032023.

[23] L. Breiman, J.H. Friedman, R.A. Olshen and C.J. Stone, *Classification and regression trees*, Wadsworth international group, Belmont, California, USA, (1984).

[24] R.E. Schapire and Y. Freund, *A decision-theoretic generalization of on-line learning and an application to boosting*, *Jour. Comp. and Syst. Sc.* **55** (1997) 119.

[25] M. Pivk and F.R. Le Diberder, *sPlot: A statistical tool to unfold data distributions*, *Nucl. Instrum. Meth.* **A 555** (2005) 356 [physics/0402083].

[26] T. Skwarnicki, *A study of the radiative cascade transitions between the Upsilon-prime and Upsilon resonances*, Ph.D. Thesis, Institute of Nuclear Physics, Krakow, Poland (1986), DESY-F31-86-02.

[27] D. Martínez Santos and F. Dupertuis, *Mass distributions marginalized over per-event errors*, *Nucl. Instrum. Meth.* **A 764** (2014) 150 [arXiv:1312.5000].

[28] LHCb collaboration, *Measurement of the CP-violating phase ϕ_s in $\bar{B}^0_s \to D^+_s D^-_s$ decays*, *Phys. Rev. Lett.* **113** (2014) 211801 [arXiv:1409.4619].

2015 JINST 10 P10005

The LHCb collaboration

R. Aaij[38], B. Adeva[37], M. Adinolfi[46], A. Affolder[52], Z. Ajaltouni[5], S. Akar[6], J. Albrecht[9], F. Alessio[38], M. Alexander[51], S. Ali[41], G. Alkhazov[30], P. Alvarez Cartelle[53], A.A. Alves Jr[57], S. Amato[2], S. Amerio[22], Y. Amhis[7], L. An[3], L. Anderlini[17], J. Anderson[40], G. Andreassi[39], M. Andreotti[16,f], J.E. Andrews[58], R.B. Appleby[54], O. Aquines Gutierrez[10], F. Archilli[38], P. d'Argent[11], A. Artamonov[35], M. Artuso[59], E. Aslanides[6], G. Auriemma[25,m], M. Baalouch[5], S. Bachmann[11], J.J. Back[48], A. Badalov[36], C. Baesso[60], W. Baldini[16,38], R.J. Barlow[54], C. Barschel[38], S. Barsuk[7], W. Barter[38], V. Batozskaya[28], V. Battista[39], A. Bay[39], L. Beaucourt[4], J. Beddow[51], F. Bedeschi[23], I. Bediaga[1], L.J. Bel[41], V. Bellee[39], N. Belloli[20], I. Belyaev[31], E. Ben-Haim[8], G. Bencivenni[18], S. Benson[38], J. Benton[46], A. Berezhnoy[32], R. Bernet[40], A. Bertolin[22], M.-O. Bettler[38], M. van Beuzekom[41], A. Bien[11], S. Bifani[45], P. Billoir[8], T. Bird[54], A. Birnkraut[9], A. Bizzeti[17,h], T. Blake[48], F. Blanc[39], J. Blouw[10], S. Blusk[59], V. Bocci[25], A. Bondar[34], N. Bondar[30,38], W. Bonivento[15], S. Borghi[54], M. Borsato[7], T.J.V. Bowcock[52], E. Bowen[40], C. Bozzi[16], S. Braun[11], M. Britsch[10], T. Britton[59], J. Brodzicka[54], N.H. Brook[46], E. Buchanan[46], A. Bursche[40], J. Buytaert[38], S. Cadeddu[15], R. Calabrese[16,f], M. Calvi[20,j], M. Calvo Gomez[36,o], P. Campana[18], D. Campora Perez[38], L. Capriotti[54], A. Carbone[14,d], G. Carboni[24,k], R. Cardinale[19,i], A. Cardini[15], P. Carniti[20], L. Carson[50], K. Carvalho Akiba[2,38], G. Casse[52], L. Cassina[20,j], L. Castillo Garcia[38], M. Cattaneo[38], Ch. Cauet[9], G. Cavallero[19], R. Cenci[23,s], M. Charles[8], Ph. Charpentier[38], M. Chefdeville[4], S. Chen[54], S.-F. Cheung[55], N. Chiapolini[40], M. Chrzaszcz[40], X. Cid Vidal[38], G. Ciezarek[41], P.E.L. Clarke[50], M. Clemencic[38], H.V. Cliff[47], J. Closier[38], V. Coco[38], J. Cogan[6], E. Cogneras[5], V. Cogoni[15,e], L. Cojocariu[29], G. Collazuol[22], P. Collins[38], A. Comerma-Montells[11], A. Contu[15,38], A. Cook[46], M. Coombes[46], S. Coquereau[8], G. Corti[38], M. Corvo[16,f], B. Couturier[38], G.A. Cowan[50], D.C. Craik[48], A. Crocombe[48], M. Cruz Torres[60], S. Cunliffe[53], R. Currie[53], C. D'Ambrosio[38], E. Dall'Occo[41], J. Dalseno[46], P.N.Y. David[41], A. Davis[57], K. De Bruyn[41], S. De Capua[54], M. De Cian[11], J.M. De Miranda[1], L. De Paula[2], P. De Simone[18], C.-T. Dean[51], D. Decamp[4], M. Deckenhoff[9], L. Del Buono[8], N. Déléage[4], M. Demmer[9], D. Derkach[55], O. Deschamps[5], F. Dettori[38], B. Dey[21], A. Di Canto[38], F. Di Ruscio[24], H. Dijkstra[38], S. Donleavy[52], F. Dordei[11], M. Dorigo[39], A. Dosil Suárez[37], D. Dossett[48], A. Dovbnya[43], K. Dreimanis[52], L. Dufour[41], G. Dujany[54], F. Dupertuis[39], P. Durante[38], R. Dzhelyadin[35], A. Dziurda[26], A. Dzyuba[30], S. Easo[49,38], U. Egede[53], V. Egorychev[31], S. Eidelman[34], S. Eisenhardt[50], U. Eitschberger[9], R. Ekelhof[9], L. Eklund[51], I. El Rifai[5], Ch. Elsasser[40], S. Ely[59], S. Esen[11], H.M. Evans[47], T. Evans[55], A. Falabella[14], C. Färber[38], C. Farinelli[41], N. Farley[45], S. Farry[52], R. Fay[52], D. Ferguson[50], V. Fernandez Albor[37], F. Ferrari[14], F. Ferreira Rodrigues[1], M. Ferro-Luzzi[38], S. Filippov[33], M. Fiore[16,38,f], M. Fiorini[16,f], M. Firlej[27], C. Fitzpatrick[39], T. Fiutowski[27], K. Fohl[38], P. Fol[53], M. Fontana[15], F. Fontanelli[19,i], R. Forty[38], O. Francisco[2], M. Frank[38], C. Frei[38], M. Frosini[17], J. Fu[21], E. Furfaro[24,k], A. Gallas Torreira[37], D. Galli[14,d], S. Gallorini[22,38], S. Gambetta[50], M. Gandelman[2], P. Gandini[55], Y. Gao[3], J. García Pardiñas[37], J. Garra Tico[47], L. Garrido[36], D. Gascon[36], C. Gaspar[38], R. Gauld[55], L. Gavardi[9], G. Gazzoni[5], D. Gerick[11], E. Gersabeck[11], M. Gersabeck[54], T. Gershon[48], Ph. Ghez[4], A. Gianelle[22], S. Gianì[39], V. Gibson[47], O. G. Girard[39], L. Giubega[29], V.V. Gligorov[38], C. Göbel[60], D. Golubkov[31], A. Golutvin[53,31,38], A. Gomes[1,a], C. Gotti[20,j], M. Grabalosa Gándara[5], R. Graciani Diaz[36], L.A. Granado Cardoso[38], E. Graugés[36], E. Graverini[40], G. Graziani[17], A. Grecu[29], E. Greening[55], S. Gregson[47], P. Griffith[45], L. Grillo[11], O. Grünberg[63], B. Gui[59], E. Gushchin[33], Yu. Guz[35,38], T. Gys[38], T. Hadavizadeh[55], C. Hadjivasiliou[59], G. Haefeli[39], C. Haen[38], S.C. Haines[47], S. Hall[53], B. Hamilton[58], X. Han[11], S. Hansmann-Menzemer[11], N. Harnew[55], S.T. Harnew[46], J. Harrison[54], J. He[38], T. Head[39], V. Heijne[41], K. Hennessy[52], P. Henrard[5], L. Henry[8], J.A. Hernando Morata[37], E. van Herwijnen[38], M. Heß[63], A. Hicheur[2], D. Hill[55], M. Hoballah[5], C. Hombach[54], W. Hulsbergen[41], T. Humair[53], N. Hussain[55], D. Hutchcroft[52], D. Hynds[51], M. Idzik[27], P. Ilten[56], R. Jacobsson[38], A. Jaeger[11], J. Jalocha[55], E. Jans[41], A. Jawahery[58], F. Jing[3], M. John[55], D. Johnson[38], C.R. Jones[47], C. Joram[38], B. Jost[38], N. Jurik[59], S. Kandybei[43], W. Kanso[6], M. Karacson[38], T.M. Karbach[38,†], S. Karodia[51],

2015 JINST 10 P10005

M. Kecke[11], M. Kelsey[59], I.R. Kenyon[45], M. Kenzie[38], T. Ketel[42], B. Khanji[20,38,j], C. Khurewathanakul[39], S. Klaver[54], K. Klimaszewski[28], O. Kochebina[7], M. Kolpin[11], I. Komarov[39], R.F. Koopman[42], P. Koppenburg[41,38], M. Kozeiha[5], L. Kravchuk[33], K. Kreplin[11], M. Kreps[48], G. Krocker[11], P. Krokovny[34], F. Kruse[9], W. Krzemien[28], W. Kucewicz[26,n], M. Kucharczyk[26], V. Kudryavtsev[34], A. K. Kuonen[39], K. Kurek[28], T. Kvaratskheliya[31], D. Lacarrere[38], G. Lafferty[54], A. Lai[15], D. Lambert[50], G. Lanfranchi[18], C. Langenbruch[48], B. Langhans[38], T. Latham[48], C. Lazzeroni[45], R. Le Gac[6], J. van Leerdam[41], J.-P. Lees[4], R. Lefèvre[5], A. Leflat[32,38], J. Lefrançois[7], O. Leroy[6], T. Lesiak[26], B. Leverington[11], Y. Li[7], T. Likhomanenko[65,64], M. Liles[52], R. Lindner[38], C. Linn[38], F. Lionetto[40], B. Liu[15], X. Liu[3], D. Loh[48], I. Longstaff[51], J.H. Lopes[2], D. Lucchesi[22,q], M. Lucio Martinez[37], H. Luo[50], A. Lupato[22], E. Luppi[16,f], O. Lupton[55], A. Lusiani[23], F. Machefert[7], F. Maciuc[29], O. Maev[30], K. Maguire[54], S. Malde[55], A. Malinin[64], G. Manca[7], G. Mancinelli[6], P. Manning[59], A. Mapelli[38], J. Maratas[5], J.F. Marchand[4], U. Marconi[14], C. Marin Benito[36], P. Marino[23,38,s], J. Marks[11], G. Martellotti[25], M. Martin[6], M. Martinelli[39], D. Martinez Santos[37], F. Martinez Vidal[66], D. Martins Tostes[2], A. Massafferri[1], R. Matev[38], A. Mathad[48], Z. Mathe[38], C. Matteuzzi[20], A. Mauri[40], B. Maurin[39], A. Mazurov[45], M. McCann[53], J. McCarthy[45], A. McNab[54], R. McNulty[12], B. Meadows[57], F. Meier[9], M. Meissner[11], D. Melnychuk[28], M. Merk[41], E Michielin[22], D.A. Milanes[62], M.-N. Minard[4], D.S. Mitzel[11], J. Molina Rodriguez[60], I.A. Monroy[62], S. Monteil[5], M. Morandin[22], P. Morawski[27], A. Mordà[6], M.J. Morello[23,s], J. Moron[27], A.B. Morris[50], R. Mountain[59], F. Muheim[50], D. Muller[54], J. Müller[9], K. Müller[40], V. Müller[9], M. Mussini[14], B. Muster[39], P. Naik[46], T. Nakada[39], R. Nandakumar[49], A. Nandi[55], I. Nasteva[2], M. Needham[50], N. Neri[21], S. Neubert[11], N. Neufeld[38], M. Neuner[11], A.D. Nguyen[39], T.D. Nguyen[39], C. Nguyen-Mau[39,p], V. Niess[5], R. Niet[9], N. Nikitin[32], T. Nikodem[11], D. Ninci[23], A. Novoselov[35], D.P. O'Hanlon[48], A. Oblakowska-Mucha[27], V. Obraztsov[35], S. Ogilvy[51], O. Okhrimenko[44], R. Oldeman[15,e], C.J.G. Onderwater[67], B. Osorio Rodrigues[1], J.M. Otalora Goicochea[2], A. Otto[38], P. Owen[53], A. Oyanguren[66], A. Palano[13,c], F. Palombo[21,t], M. Palutan[18], J. Panman[38], A. Papanestis[49], M. Pappagallo[51], L.L. Pappalardo[16,f], C. Pappenheimer[57], C. Parkes[54], G. Passaleva[17], G.D. Patel[52], M. Patel[53], C. Patrignani[19,i], A. Pearce[54,49], A. Pellegrino[41], G. Penso[25,l], M. Pepe Altarelli[38], S. Perazzini[14,d], P. Perret[5], L. Pescatore[45], K. Petridis[46], A. Petrolini[19,i], M. Petruzzo[21], E. Picatoste Olloqui[36], B. Pietrzyk[4], T. Pilař[48], D. Pinci[25], A. Pistone[19], A. Piucci[11], S. Playfer[50], M. Plo Casasus[37], T. Poikela[38], F. Polci[8], A. Poluektov[48,34], I. Polyakov[31], E. Polycarpo[2], A. Popov[35], D. Popov[10,38], B. Popovici[29], C. Potterat[2], E. Price[46], J.D. Price[52], J. Prisciandaro[39], A. Pritchard[52], C. Prouve[46], V. Pugatch[44], A. Puig Navarro[39], G. Punzi[23,r], W. Qian[4], R. Quagliani[7,46], B. Rachwal[26], J.H. Rademacker[46], M. Rama[23], M.S. Rangel[2], I. Raniuk[43], N. Rauschmayr[38], G. Raven[42], F. Redi[53], S. Reichert[54], M.M. Reid[48], A.C. dos Reis[1], S. Ricciardi[49], S. Richards[46], M. Rihl[38], K. Rinnert[52], V. Rives Molina[36], P. Robbe[7,38], A.B. Rodrigues[1], E. Rodrigues[54], J.A. Rodriguez Lopez[62], P. Rodriguez Perez[54], S. Roiser[38], V. Romanovsky[35], A. Romero Vidal[37], J. W. Ronayne[12], M. Rotondo[22], J. Rouvinet[39], T. Ruf[38], H. Ruiz[36], P. Ruiz Valls[66], J.J. Saborido Silva[37], N. Sagidova[30], P. Sail[51], B. Saitta[15,e], V. Salustino Guimaraes[2], C. Sanchez Mayordomo[66], B. Sanmartin Sedes[37], R. Santacesaria[25], C. Santamarina Rios[37], M. Santimaria[18], E. Santovetti[24,k], A. Sarti[18,l], C. Satriano[25,m], A. Satta[24], D.M. Saunders[46], D. Savrina[31,32], M. Schiller[38], H. Schindler[38], M. Schlupp[9], M. Schmelling[10], T. Schmelzer[9], B. Schmidt[38], O. Schneider[39], A. Schopper[38], M. Schubiger[39], M.-H. Schune[7], R. Schwemmer[38], B. Sciascia[18], A. Sciubba[25,l], A. Semennikov[31], N. Serra[40], J. Serrano[6], L. Sestini[22], P. Seyfert[20], M. Shapkin[35], I. Shapoval[16,43,f], Y. Shcheglov[30], T. Shears[52], L. Shekhtman[34], V. Shevchenko[64], A. Shires[9], B.G. Siddi[16], R. Silva Coutinho[48], L. Silva de Oliveira[2], G. Simi[22], M. Sirendi[47], N. Skidmore[46], I. Skillicorn[51], T. Skwarnicki[59], E. Smith[55,49], E. Smith[53], I. T. Smith[50], J. Smith[47], M. Smith[54], H. Snoek[41], M.D. Sokoloff[57,38], F.J.P. Soler[51], F. Soomro[39], D. Souza[46], B. Souza De Paula[2], B. Spaan[9], P. Spradlin[51], S. Sridharan[38], F. Stagni[38], M. Stahl[11], S. Stahl[38], S. Stefkova[53], O. Steinkamp[40], O. Stenyakin[35], S. Stevenson[55], S. Stoica[29], S. Stone[59], B. Storaci[40], S. Stracka[23,s], M. Straticiuc[29], U. Straumann[40], L. Sun[57], W. Sutcliffe[53], K. Swientek[27], S. Swientek[9], V. Syropoulos[42], M. Szczekowski[28], P. Szczypka[39,38],

2015 JINST 10 P10005

T. Szumlak[27], S. T'Jampens[4], A. Tayduganov[6], T. Tekampe[9], M. Teklishyn[7], G. Tellarini[16,f], F. Teubert[38], C. Thomas[55], E. Thomas[38], J. van Tilburg[41], V. Tisserand[4], M. Tobin[39], J. Todd[57], S. Tolk[42], L. Tomassetti[16,f], D. Tonelli[38], S. Topp-Joergensen[55], N. Torr[55], E. Tournefier[4], S. Tourneur[39], K. Trabelsi[39], M.T. Tran[39], M. Tresch[40], A. Trisovic[38], A. Tsaregorodtsev[6], P. Tsopelas[41], N. Tuning[41,38], A. Ukleja[28], A. Ustyuzhanin[65,64], U. Uwer[11], C. Vacca[15,e], V. Vagnoni[14], G. Valenti[14], A. Vallier[7], R. Vazquez Gomez[18], P. Vazquez Regueiro[37], C. Vázquez Sierra[37], S. Vecchi[16], J.J. Velthuis[46], M. Veltri[17,g], G. Veneziano[39], M. Vesterinen[11], B. Viaud[7], D. Vieira[2], M. Vieites Diaz[37], X. Vilasis-Cardona[36,o], A. Vollhardt[40], D. Volyanskyy[10], D. Voong[46], A. Vorobyev[30], V. Vorobyev[34], C. Voß[63], J.A. de Vries[41], R. Waldi[63], C. Wallace[48], R. Wallace[12], J. Walsh[23], S. Wandernoth[11], J. Wang[59], D.R. Ward[47], N.K. Watson[45], D. Websdale[53], A. Weiden[40], M. Whitehead[48], G. Wilkinson[55,38], M. Wilkinson[59], M. Williams[38], M.P. Williams[45], M. Williams[56], T. Williams[45], F.F. Wilson[49], J. Wimberley[58], J. Wishahi[9], W. Wislicki[28], M. Witek[26], G. Wormser[7], S.A. Wotton[47], S. Wright[47], K. Wyllie[38], Y. Xie[61], Z. Xu[39], Z. Yang[3], J. Yu[61], X. Yuan[34], O. Yushchenko[35], M. Zangoli[14], M. Zavertyaev[10,b], L. Zhang[3], Y. Zhang[3], A. Zhelezov[11], A. Zhokhov[31], L. Zhong[3], S. Zucchelli[14].

[1] *Centro Brasileiro de Pesquisas Físicas (CBPF), Rio de Janeiro, Brazil*
[2] *Universidade Federal do Rio de Janeiro (UFRJ), Rio de Janeiro, Brazil*
[3] *Center for High Energy Physics, Tsinghua University, Beijing, China*
[4] *LAPP, Université Savoie Mont-Blanc, CNRS/IN2P3, Annecy-Le-Vieux, France*
[5] *Clermont Université, Université Blaise Pascal, CNRS/IN2P3, LPC, Clermont-Ferrand, France*
[6] *CPPM, Aix-Marseille Université, CNRS/IN2P3, Marseille, France*
[7] *LAL, Université Paris-Sud, CNRS/IN2P3, Orsay, France*
[8] *LPNHE, Université Pierre et Marie Curie, Université Paris Diderot, CNRS/IN2P3, Paris, France*
[9] *Fakultät Physik, Technische Universität Dortmund, Dortmund, Germany*
[10] *Max-Planck-Institut für Kernphysik (MPIK), Heidelberg, Germany*
[11] *Physikalisches Institut, Ruprecht-Karls-Universität Heidelberg, Heidelberg, Germany*
[12] *School of Physics, University College Dublin, Dublin, Ireland*
[13] *Sezione INFN di Bari, Bari, Italy*
[14] *Sezione INFN di Bologna, Bologna, Italy*
[15] *Sezione INFN di Cagliari, Cagliari, Italy*
[16] *Sezione INFN di Ferrara, Ferrara, Italy*
[17] *Sezione INFN di Firenze, Firenze, Italy*
[18] *Laboratori Nazionali dell'INFN di Frascati, Frascati, Italy*
[19] *Sezione INFN di Genova, Genova, Italy*
[20] *Sezione INFN di Milano Bicocca, Milano, Italy*
[21] *Sezione INFN di Milano, Milano, Italy*
[22] *Sezione INFN di Padova, Padova, Italy*
[23] *Sezione INFN di Pisa, Pisa, Italy*
[24] *Sezione INFN di Roma Tor Vergata, Roma, Italy*
[25] *Sezione INFN di Roma La Sapienza, Roma, Italy*
[26] *Henryk Niewodniczanski Institute of Nuclear Physics Polish Academy of Sciences, Kraków, Poland*
[27] *AGH - University of Science and Technology, Faculty of Physics and Applied Computer Science, Kraków, Poland*
[28] *National Center for Nuclear Research (NCBJ), Warsaw, Poland*
[29] *Horia Hulubei National Institute of Physics and Nuclear Engineering, Bucharest-Magurele, Romania*
[30] *Petersburg Nuclear Physics Institute (PNPI), Gatchina, Russia*
[31] *Institute of Theoretical and Experimental Physics (ITEP), Moscow, Russia*
[32] *Institute of Nuclear Physics, Moscow State University (SINP MSU), Moscow, Russia*
[33] *Institute for Nuclear Research of the Russian Academy of Sciences (INR RAN), Moscow, Russia*
[34] *Budker Institute of Nuclear Physics (SB RAS) and Novosibirsk State University, Novosibirsk, Russia*
[35] *Institute for High Energy Physics (IHEP), Protvino, Russia*
[36] *Universitat de Barcelona, Barcelona, Spain*
[37] *Universidad de Santiago de Compostela, Santiago de Compostela, Spain*

2015 JINST 10 P10005

[38] European Organization for Nuclear Research (CERN), Geneva, Switzerland
[39] Ecole Polytechnique Fédérale de Lausanne (EPFL), Lausanne, Switzerland
[40] Physik-Institut, Universität Zürich, Zürich, Switzerland
[41] Nikhef National Institute for Subatomic Physics, Amsterdam, The Netherlands
[42] Nikhef National Institute for Subatomic Physics and VU University Amsterdam, Amsterdam, The Netherlands
[43] NSC Kharkiv Institute of Physics and Technology (NSC KIPT), Kharkiv, Ukraine
[44] Institute for Nuclear Research of the National Academy of Sciences (KINR), Kyiv, Ukraine
[45] University of Birmingham, Birmingham, United Kingdom
[46] H.H. Wills Physics Laboratory, University of Bristol, Bristol, United Kingdom
[47] Cavendish Laboratory, University of Cambridge, Cambridge, United Kingdom
[48] Department of Physics, University of Warwick, Coventry, United Kingdom
[49] STFC Rutherford Appleton Laboratory, Didcot, United Kingdom
[50] School of Physics and Astronomy, University of Edinburgh, Edinburgh, United Kingdom
[51] School of Physics and Astronomy, University of Glasgow, Glasgow, United Kingdom
[52] Oliver Lodge Laboratory, University of Liverpool, Liverpool, United Kingdom
[53] Imperial College London, London, United Kingdom
[54] School of Physics and Astronomy, University of Manchester, Manchester, United Kingdom
[55] Department of Physics, University of Oxford, Oxford, United Kingdom
[56] Massachusetts Institute of Technology, Cambridge, MA, United States
[57] University of Cincinnati, Cincinnati, OH, United States
[58] University of Maryland, College Park, MD, United States
[59] Syracuse University, Syracuse, NY, United States
[60] Pontifícia Universidade Católica do Rio de Janeiro (PUC-Rio), Rio de Janeiro, Brazil, associated to [2]
[61] Institute of Particle Physics, Central China Normal University, Wuhan, Hubei, China, associated to [3]
[62] Departamento de Fisica , Universidad Nacional de Colombia, Bogota, Colombia, associated to [8]
[63] Institut für Physik, Universität Rostock, Rostock, Germany, associated to [11]
[64] National Research Centre Kurchatov Institute, Moscow, Russia, associated to [31]
[65] Yandex School of Data Analysis, Moscow, Russia, associated to [31]
[66] Instituto de Fisica Corpuscular (IFIC), Universitat de Valencia-CSIC, Valencia, Spain, associated to [36]
[67] Van Swinderen Institute, University of Groningen, Groningen, The Netherlands, associated to [41]

[a] Universidade Federal do Triângulo Mineiro (UFTM), Uberaba-MG, Brazil
[b] P.N. Lebedev Physical Institute, Russian Academy of Science (LPI RAS), Moscow, Russia
[c] Università di Bari, Bari, Italy
[d] Università di Bologna, Bologna, Italy
[e] Università di Cagliari, Cagliari, Italy
[f] Università di Ferrara, Ferrara, Italy
[g] Università di Urbino, Urbino, Italy
[h] Università di Modena e Reggio Emilia, Modena, Italy
[i] Università di Genova, Genova, Italy
[j] Università di Milano Bicocca, Milano, Italy
[k] Università di Roma Tor Vergata, Roma, Italy
[l] Università di Roma La Sapienza, Roma, Italy
[m] Università della Basilicata, Potenza, Italy
[n] AGH - University of Science and Technology, Faculty of Computer Science, Electronics and Telecommunications, Kraków, Poland
[o] LIFAELS, La Salle, Universitat Ramon Llull, Barcelona, Spain
[p] Hanoi University of Science, Hanoi, Viet Nam
[q] Università di Padova, Padova, Italy
[r] Università di Pisa, Pisa, Italy
[s] Scuola Normale Superiore, Pisa, Italy
[t] Università degli Studi di Milano, Milano, Italy

[†] Deceased

2015 JINST 10 P10005